https://doi.org/10.5194/hess-2022-375
Preprint. Discussion started: 16 January 2023

Hydrology and Earth System Sciences
Discussions
Open Access
EGU

Hydrological effects of evapotranspiration in the Qilian Mountains forest belt

Yinying Jiao[1,2], Guofeng Zhu[1,2*], Dongdong Qiu[1,2], Yuwei Liu[1,2], Lei Wang[1,2], Siyu Lu[1,2], Gaojia Meng[1,2], Xinrui Lin[1,2], Rui Li[1,2], Qinqin Wang[1,2], Longhu Chen[1,2], Niu Sun[1,2]

[1] School of Geography and Environment Science, Northwest Normal University, Lanzhou 730070, Gansu, China

[2] Shiyang River Ecological Environment Observation Station, Northwest Normal University, Lanzhou 730070, Gansu, China

Abstract: Mountainous areas are the main water-producing and source areas of rivers. Global climate change is transforming the distribution of plants and forms of water use. Therefore, a clear understanding of evapotranspiration in mountainous forest zone is key for understanding the ecohydrological effect of vegetation and its influence on the water cycle of the watershed. We quantified the evapotranspiration processes in the forest belts of the Qilian Mountains as well as their contribution to runoff yield and concentration based on precipitation, soil water, and plant water samples and experimental data. The study showed that transpiration of Qinghai spruce accounted for the highest proportion of evapotranspiration in the entire Qinghai spruce forest ecosystem, with an average of 79%, which means that transpiration is much greater than evaporation. Soil water content and air humidity were the dominant factors influencing evapotranspiration in Qinghai spruce forest belts. The growing season of Qinghai spruce is characterized by greater evapotranspiration than precipitation in each month. Consequently, the forest zone does not yield flows in the eastern part of the Qilian Mountains. The warming of global temperatures and human activities are likely to trigger shifts in the distribution areas and evapotranspiration regimes of Qinghai spruce, which in turn will lead to a change in water resource patterns in the basin.

https://doi.org/10.5194/hess-2022-375
Preprint. Discussion started: 16 January 2023

Hydrology and Earth System Sciences
Discussions

Keywords: Qinghai spruce; stable isotopes; end-member mixing model; evapotranspiration partitioning

1. Introduction

Future droughts are likely to be more frequent, more severe, and longer-lasting than in recent decades. These changes are expected to be most rapid and extreme in ecologically fragile areas, especially in ecosystems in arid and semi-arid regions (Ault et al., 2020). As a vascular plant species, Qinghai spruce forests are one of the important entry points for energy and materials in the environment into terrestrial ecosystems. Their growth, survival, and reproduction affect other species' ecological functions and forms within and outside their habitats. There is a high degree of responsiveness between the vegetation, drought resilience, and microclimatic conditions of forests and their ecosystems (Eisenhauer et al., 2021). The spruce forest ecosystem provides various ecological, climatic, and social benefits to the Qilian Mountains but is highly vulnerable to drought and temperature extremes. More to the point, climate drivers put spruce forests at risk from drought and heat stress. As the magnitude of climate change increases, the disturbance to its ecosystem is also expected to be higher. It is an important player in climate change mitigation in terms of climate benefits (Rohatyn et al., 2022). At the ecosystem scale, many studies have classified evapotranspiration (ET) as transpiration (T) and evapotranspiration (E) (Schlesinger et al.,2014). Physical evaporation from the soil surface and biological transpiration (involving soil water uptake by roots and water vapour loss through plant stomata during photosynthesis) have become bases for classifying ET in field research. Some studies have classified E and T by measuring the isotopic composition of oxygen in soil and runoff and concluded that $\delta^{18}O$ is enriched by evaporation rather than transpiration (Wershaw et al., 1966). Dividing evapotranspiration (ET) into soil evaporation (E) and stomatal plant evapotranspiration (T) is challenging but important for assessing biomass production and allocating increasingly scarce water resources. Typically, T is the desired component of water used to enhance plant productivity, while E is considered a source of water loss or inefficiency. The magnitude of E is expected to be remarkable in sparsely vegetated systems, particularly in arid areas or very wet systems (e.g., surface irrigated crops and wetlands)(Liu et al., 2015;Zhang et al., 2018). ET zoning is fundamental for the accurate monitoring of system hydrology and improved water management practices in these cases (Kool et al.,2014). It is, therefore, critical to quantify the role of regional evapotranspiration in the terrestrial water balance and the global water cycle.

On the regional and global scales, there are many methods to divide evapotranspiration. Mainly have (1) river basins, where the role of lateral groundwater flow in evapotranspiration distribution is investigated by using a comprehensive continental scale hydrological model, and the vegetation and land energy processes are coupled with surface and underground hydrology to study the continental scale evapotranspiration distribution (Maxwell et al.,2016). (2) remote sensing-based approaches to reveal differences in ET partitioning across models (Talsma et al., 2018; Chen et al.,2022); (3) the use of eddy covariance methods to assess multi-year energy fluxes and ET in typical alpine meadows and their environmental and biophysical controls (Chang et al.,2022), as well as studies that synthesize all available literature data in an attempt to establish quantitative relationships between ET allocation and vegetation cover indices (e.g. LAI) for agricultural and natural systems, and to explain observed changes in T/ET at global scales (Wang et al., 2014;Wei et al., 2018; Cui et al., 2021).

As a water source for several inland rivers, the Qilian Mountains are an important ecological security barrier and a priority area for biodiversity conservation in central Asia. We observed and analyzed month-by-month xylem water, soil water, stable precipitation isotopes, and soil water content of Qinghai spruce forests in the eastern part of the Qilian Mountains from April to October 2019. The seasonal variation of water isotopes in different sources of water bodies was first determined, and the composition and variation of oxygen isotopes in soil evaporation, plant transpiration, and ecosystem evapotranspiration were analyzed. Later, the evapotranspiration fluxes were divided into transpiration and evapotranspiration, and

https://doi.org/10.5194/hess-2022-375
Preprint. Discussion started: 16 January 2023

then the hydrological effects of evapotranspiration were analysed. This study provides an effective basis for local water resource use and ecological protection.

2. Study area

The Qilian Mountains are a system of marginal mountains in the northeastern part of the Qinghai-Tibet Plateau. It lies between 94°E~104°E and 36°N~39°N, straddling the Qinghai-Gansu provinces, starting from the Dangjinshan Pass in the west and reaching the Wushaoling in the east, adjacent to the Qaidam Basin, the Chaka-Gonghe Basin and the Yellow River Valley in the south, and the Hexi Corridor in the north. The Shiyang River basin is located in the east of the Qilian Mountain, with a high terrain in the south and low terrain in the north, and it slopes from southwest to northeast. The basin can be divided into four geomorphological units: the Qilian Mountains in the south, the plains of the central corridor, the low hills in the north and the desert area (Zhu et al., 2019). The study area is located in the upper reaches of Xiying River at an altitude of 2700 m, which is the largest tributary of the Shiyang River and belongs to the south Qilian Mountains. It is considered an alpine semiarid and semi-humid zone with annual precipitation of 469.44 mm, annual evaporation of 700-1200 mm, and an average annual temperature of 3.24°C (Zhu et al., 2022).

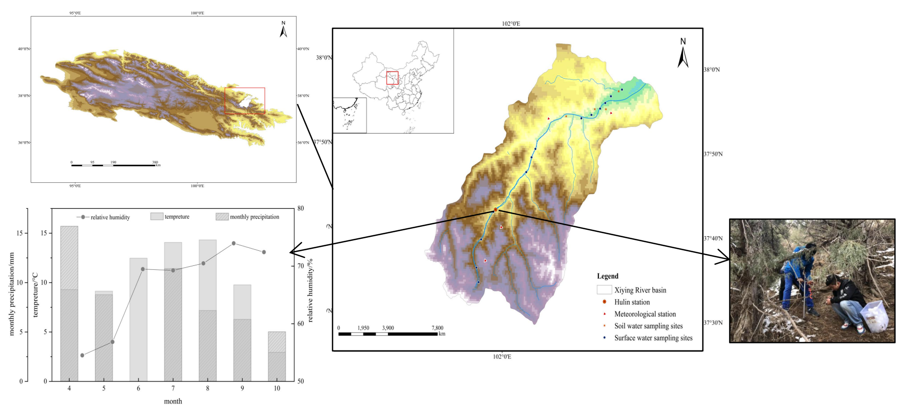

Figure 1 Location of the study area and changes in meteorological elements.

https://doi.org/10.5194/hess-2022-375
Preprint. Discussion started: 16 January 2023

3. Materials and methods

3.1 Materials Sources

Water isotopes in precipitation, vegetation, and soil water were observed at the Xiying River Basin Ranger Station (101°53′E, 37°41′N; 2721 m asl) from April to October 2019, and temperature, precipitation, and relative humidity data were obtained using the station's meteorological recorder. The monthly potential evapotranspiration data of 1 km in China (1990-2021) with a spatial resolution of 0.0083333 °（Peng et al.,2022;Dinget al.,2020;Ding et al.,2021）. The surface evapotranspiration data were obtained from the MODIS-based daily surface evapotranspiration data of the Qilian Mountains (2019), with a spatial resolution of 0.01°（Yao et al., 2017;Yao et al., 2020）.

3.2 Research methods

3.2.1 Isotopic composition of atmospheric water vapour

The stable isotope composition of moisture in ambient air is calculated as follows:

$$\delta_A = \frac{\delta_{rain} - k\varepsilon^+}{1 + k\alpha^+ \times 10^{-3}} \qquad (1)$$

where k=1, or by fitting k to some fraction of 1 as the best fit to the local evaporation line, is the isotopic fractionation factor. Defined by $\varepsilon^+ = (\alpha^+ - 1) \times 1000$。$\alpha^+$about ^{2}H and ^{18}O are calculated as follows:

$$10^3 ln^2\alpha^+ = 1158.8T^3/10^9 - 1620.1T^2/10^6 + 794.84T/10^3 - 161.04 + 2.9992 \times 10^9/T^3 \qquad (2)$$

$$10^3 ln^{18}\alpha^+ =- 7.685 + 6.712310^3 /T - 1.6664\times 10^6 /T^2 + 0.35041 \times 10^9/ T^3 \qquad (3)$$

3.3.2 Isotopic composition of soil evaporation

The Craig-Gordon model was used to calculate the stable isotopic composition of soil evaporation water vapour, δ_E, using the following equation:

https://doi.org/10.5194/hess-2022-375
Preprint. Discussion started: 16 January 2023

Hydrology and Earth System Sciences
Open Access
EGU
Discussions

$$\delta_E = \frac{\alpha_e^{-1}\delta_s - h^*\delta_v - \varepsilon_{eq} - (1-h^*)\varepsilon_k}{(1-h^*)+10^{-3}(1-h^*)\varepsilon_k} \qquad (4)$$

where α_e(>1) is the equilibrium factor calculated as a function of water surface temperature, δ_s is the stable isotopic composition of liquid water at the evaporating surface of the soil (0 ~ 10 cm average stable isotopic composition of soil water), δ_v is the stable isotopic composition of atmospheric water vapour near the surface, εeq represents the equilibrium fractionation corresponding to $\varepsilon_{eq} = (1\text{-}1/\alpha e) \times 1000$, ε_k is the kinetic fractionation factor of O_2 is approximately 18. 9‰ and h^* is the atmospheric relative humidity. For $\delta^{18}O$, αe is calculated as follows.

$$\alpha_e = \frac{1.137\times10^6/T^2 - 0.4156\times10^3/T - 2.0667}{1000} + 1 \qquad (5)$$

where: T is the soil Kelvin temperature (K) at a depth of 5 cm.

3.3.3 Isotopic composition of plant transpiration

When transpiration is high, plant leaf water is "isotopically stable", i.e. the isotopic composition of leaf transpiration water is equal to the isotopic composition of water absorbed by the root system during noon of the rain plant. The plant xylem water stable isotopic composition can therefore be used to represent the plant transpiration water vapour stable isotopic composition, i.e:

$$\delta_T = \delta_X \qquad (6)$$

where δ_x is the isotopic ratio of xylem water and δ_T is the isotopic ratio of transpiration.

3.3.4 Evapotranspiration isotope assessment

The Keeling Plot model describes the linear relationship between the oxygen isotope composition of atmospheric water vapour and its reciprocal concentration(Keeling et al., 1958). The intercept of the curve on the Y-axis represents the isotopic composition of evapotranspiration oxygen (δ_{ET}) and is expressed as：

$$\delta_b = \frac{C_a(\delta_a - \delta_{ET})}{C_b} + \delta_{ET} \qquad (7)$$

Where δ_b and C_b represent the atmospheric water vapour oxygen isotopic composition (‰) and water vapour concentration in the ecosystem boundary layer, δ_a and C_a represent the background atmospheric water vapour oxygen isotopic composition and background atmospheric water vapour concentration, and δ_{ET} is the ecosystem evapotranspiration oxygen isotopic composition.

3.3.5 Ecosystem evapotranspiration partitioning

The determination of evapotranspiration by means of biotic and abiotic isotopic water fluxes can be used to improve the understanding of community structure and ecosystem function in Qinghai spruce forests in the Qilian Mountains. Based on the isotope mass balance approach to consider the distribution of major and minor isotopes, the partitioning of evapotranspiration can be achieved using two end-member mixing models (E and T) with the following expression:

$$\frac{T}{ET} = \frac{\delta_{ET}-\delta_E}{\delta_T-\delta_E} \qquad (8)$$

where δ_{ET}, δ_E and δ_T are the isotopic compositions of evapotranspiration (ET), soil evapotranspiration (E) and plant evapotranspiration (T), respectively, and the isotopic values of the three can be obtained by both direct observation and model estimation.

Their respective contributions can be calculated by the following equations:

$$f_E = \frac{\delta_{ET}-\delta_T}{\delta_E-\delta_T} \times 100\% \qquad (9)$$

$$f_T = \frac{\delta_{ET}-\delta_E}{\delta_T-\delta_E} \times 100\% \qquad (10)$$

3.3.6 Three-component mixing model

Assuming that the water vapour in precipitation is a mixture of advective water vapour and recirculating water vapour, it is understood that the proportion of both precipitation and precipitation water vapour has the same nature. The proportion of precipitation occupied by circulating water vapour is calculated as follow:

$$f_{re} = \frac{P_{tr}+P_{ev}}{P_{tr}+P_{ev}+P_{adv}} \qquad (9)$$

where P_{tr}, P_{ev} and P_{adv} are precipitation produced by transpiration, surface evaporation and advection, respectively.

This can be calculated using the following formula:

https://doi.org/10.5194/hess-2022-375
Preprint. Discussion started: 16 January 2023

Hydrology and Earth System Sciences
Discussions

$$\delta_{pv} = \delta_{tr} f_{tr} + \delta_{ev} f_{ev} + \delta_{adv} f_{adv} \quad (10)$$

$$f_{ev} + f_{tv} + f_{adv} = 1 \quad (11)$$

where f_{tr}, f_{ev} and f_{adv} are the proportional contributions of transpiration, surface evaporation and advection to precipitation, respectively, and δ_{pv}, δ_{tr}, δ_{ev} and δ_{adv} values are the stable isotopes in precipitating transpiration, transpiration, surface evaporation and advective vapour, respectively.

4. Results and analysis

4.1 Hydrogen and oxygen isotope variations in different water bodies

The hydrogen and oxygen isotope compositions of different sources of water (precipitation, soil water, and plant xylem water) in the study area from April to October were selected for comparison with the global atmospheric water line (Fig. 2a). It can be seen that the local atmospheric water line is close to the global atmospheric water line in terms of linear tilt rate, their linear equations are respectively $\delta^2H=7.51\delta^{18}O+10.77$, $R^2=0.97$ and $\delta^2H=8\delta^{18}O+10$. Local precipitation $\delta^{18}O$ values varied from -20.30‰ to -0.62‰, with an average value of -7.79‰, and δ^2H values varied from -137.74‰ to 3.29‰, with an average value of -47.67‰. The hydrogen and oxygen isotope values of soil water in each soil layer are mostly distributed below the local atmospheric waterline. The range and mean values of $\delta^{18}O$ variation were -8.75‰~-4.35‰, -6.18‰. The range and mean values of δ^2H were -58.43‰ to -28.26‰ and -42.08‰. This indicates that soil moisture is mainly affected by atmospheric precipitation. The soil waterline equation is δ^2H= 6.06δ18O-4.61, $R^2=0.83$, and its linear tilt and intercept were smaller than LMWL due to slight evaporation from the soil. Table 1 shows the water isotope sampling sites of Qinghai spruce xylem in the study area, and the water line equation was $\delta^2H=1.03\delta^{18}O-32.47$.

Table 1 Stable isotope composition of different water bodies.

Types	δ^2H/‰			$\delta^{18}O$/‰			Number of Samples
	max	min	average	max	min	average	

https://doi.org/10.5194/hess-2022-375
Preprint. Discussion started: 16 January 2023

Soil water	-4.54	-58.43	-31.60	-4.35	-52.93	-16.66	41
Xylem water	-24.12	-40.53	-34.42	8.45	-6.72	-1.90	7
Precipitation	3.29	-137.74	-47.67	-0.62	-20.30	-7.79	43

Rainfall in the study area was concentrated during the vegetative growth period (Fig. 2b). Both the precipitation amounts and the $\delta^{18}O$ values were higher in mid-to-late April, reaching a maximum of 27.4 mm on April 28, and lower values in May and June compared to other months. $\delta^{18}O$ was at a maximum of -0.62‰. It is clearly seen that the precipitation $\delta^{18}O$ varies from June to October with a trend of increasing and then decreasing. The oxygen isotopes of shallow soil water (0 ~ 10cm) and xylem water were higher in the middle and late April, which were -4.91 ‰ and 8.45 ‰, respectively, but fluctuated greatly in the monsoon season. The $\delta^{18}O$ of shallow soil water peaked in late June with a maximum value of -4.35‰, and the $\delta^{18}O$ maximum of xylem water occurred in late April with a maximum value of 8.45‰. Soil water content was higher in August than in May, as was the intensity of soil evaporation. In terms of the layer profile, soil water content showed a trend of increasing and then decreasing on a vertical gradient in all three months (Fig.3a).

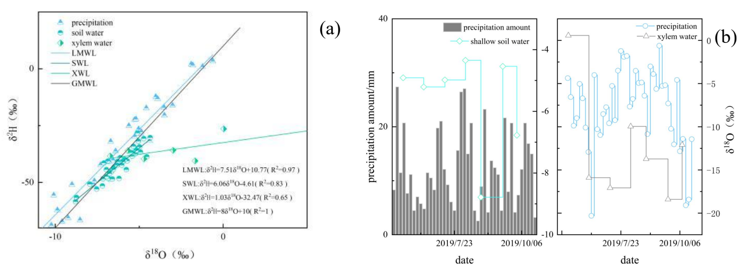

Figure 2 (a) Hydrogen and oxygen stable isotope linkages, (b) Precipitation and oxygen isotope changes in different water bodies.

Atmospheric water vapour stable isotopes were calculated based on stable precipitation isotopes (Fig. 3b), with an average atmospheric water vapour $\delta^{18}O$ of -8.15‰, with the smallest initial value of -20.41‰ in May and a maximum value of -1.34‰ in late July. The average atmospheric water vapour δ^2H was -49.69‰, fluctuating from -131.79‰ to 1.59 (Table 1). The average deuterium surplus from

https://doi.org/10.5194/hess-2022-375
Preprint. Discussion started: 16 January 2023

Hydrology and Earth System Sciences
Open Access
Discussions

April to October is 14.62‰, reaching a maximum value of 30.95‰ in early May, indicating high atmospheric humidity. After which, the deuterium value falls rapidly to its lower limit of 1.57‰ in early July. Deuterium values fluctuated slowly from June to August and began to fluctuate significantly from the middle of August, indicating that local evaporation was influenced by temperature and relative humidity over time, which made evaporation gradually stronger and unbalanced evaporation gradually stronger.

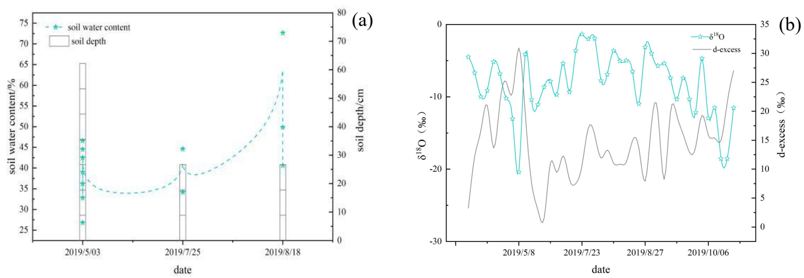

Figure 3 (a) Variation in soil water content, (b) Comparison between atmospheric water vapour oxygen isotopes and d-excess

4.2 Soil evaporation, plant transpiration and ecosystem evapotranspiration

The Craig-Gordon model and the steady-state isotopic assumption were used to derive the oxygen isotopic composition of soil evaporation and plant transpiration (Fig. 4a), respectively. The Keeling Plot model method was used to obtain the oxygen isotopic composition of ecosystem evapotranspiration (Fig. 4b). According to the results shown in the figure, the changes of oxygen isotope composition in the three water bodies from April to October were compared. The overall magnitude pattern was: $\delta^{18}O_X > \delta^{18}O_{ET} > \delta^{18}O_E$. The fluctuations of $\delta^{18}O_X$ and $\delta^{18}O_E$ were roughly parallel to each other on the horizontal time axis, but the plant transpiration oxygen isotope fluctuations were more dramatic than the soil evaporation oxygen isotope compositions, reaching the lowest values in June and September, respectively. From April to October, the mean value of soil evaporation oxygen isotope was -121.87‰, and the mean value of plant transpiration oxygen isotope was -1.90‰. This would

https://doi.org/10.5194/hess-2022-375
Preprint. Discussion started: 16 January 2023

Hydrology and Earth System Sciences
Discussions

suggest that all three are consistently affected by seasonal changes. Compared with the oxygen isotopic composition of soil evaporation, the isotopic composition of shallow soil water is shown as follows: $\delta^{18}O_S > \delta^{18}O_E$ (Fig. 5a). It shows that the fluctuation changes of the two are not consistent, but the $\delta^{18}O$ values are decreasing in general. These results indicated that the isotope fractionation of soil water occurred during the evaporation process, soil surface liquid water oxygen isotopes were visibly enriched and conversely, soil evaporation oxygen isotope composition underwent obvious depletion.

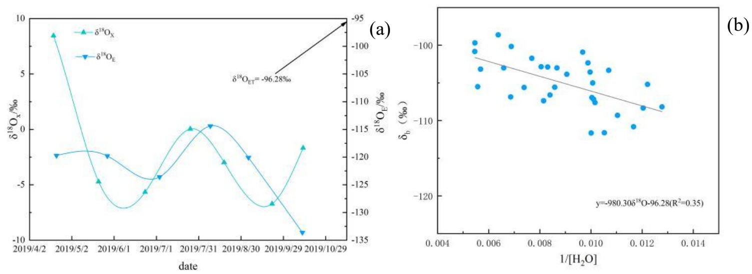

Figure 4 Isotopic composition of soil evaporation, plant transpiration and ecosystem evapotranspiration (a) and (b)

4.3 T/ET assessment of Qinghai spruce forest ecosystem in different months

The contribution of plant transpiration to evapotranspiration (T/ET) from April to October was calculated, combined with the $\delta^{18}O$ values of plant xylem water and shallow layer (0-10cm) during the same period (Fig. 5b). The T/ET values are gradually increasing before the onset of summer winds, showing a slight increase in the range of 0.15 to 0.20. The mean oxygen isotope values of xylem water and shallow soil water from April to June were respectively 1.87‰ and -4.95‰, indicating that the response of transpiration to temperature change was higher than that of shallow soil water evaporation during this period. It directly proved that the increase in T/ET value is attributed to transpiration. In the summer wind-influenced season, T/ET fluctuates between 0.15 and 0.25 slightly, and the water-oxygen isotope

https://doi.org/10.5194/hess-2022-375
Preprint. Discussion started: 16 January 2023

values of the xylem are generally higher than those of the shallow soil water-oxygen isotope values from July to August. In this period, the spruce forest was subjected to good rain and heat conditions, the surface soil layer less inhibited soil evaporation, and the soil water absorbed by the root area of the forest was more abundant. Therefore, evaporation and transpiration were more intense in this period, which showed an obvious transpiration season. From September to October, the T/ET ratio fluctuated between 0.20 and 0.30, and its average value was greater during this period compared with the summer wind-influenced period. This represented a strong surface resistance to soil evaporation when climatic conditions are not favorable, despite the fact that soil water satisfies transpiration in the root zone, resulting in lower E values and increased T/ET values. The $\delta^{18}O$ values of xylem water and shallow soil water were -4.20‰ and -5.66‰, respectively, which means that the transpiration of spruce forest trees was more intense.A month-by-month comparison of the two contributions to evapotranspiration (Fig. 5c) showed that the plant transpiration contribution f_T ranged from 0.70% to 0.85% during the study period, while the soil evapotranspiration contribution only ranged from 0.15% to 0.35%, with the former significantly higher than the latter in all months. $f_{T.}$ From April to October, the mean value of f_T was 79%, and the mean value of f_E was 20%. The mean values of f_T and f_E from April to October were 79% and 20%, respectively, indicating that the evapotranspiration of the Qinghai spruce forest ecosystem was mainly composed of transpiration from forest trees.

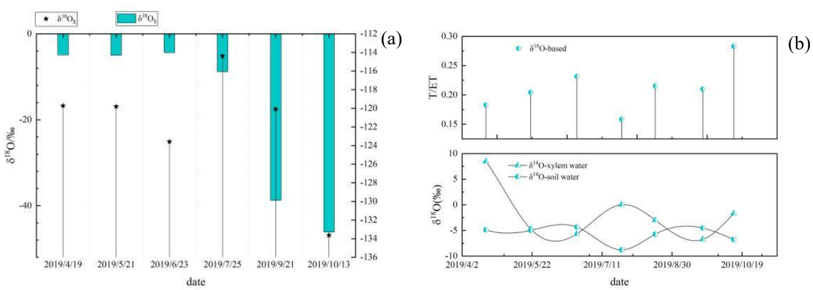

https://doi.org/10.5194/hess-2022-375
Preprint. Discussion started: 16 January 2023

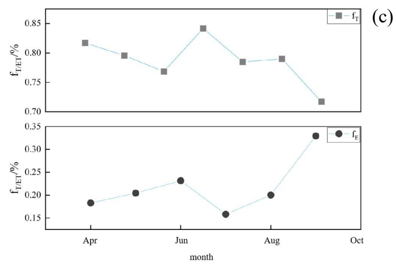

Figure 5 (a) Isotopic composition of water oxygen in shallow soils versus isotopic composition of evaporative oxygen in soils, (b) Effect of biotic and abiotic components of ecosystems on evapotranspiration in different seasons, (c) Contribution of T and E to evapotranspiration

5. Discussions

5.1 Hydrological effects of changes in evapotranspiration

5.1.1 Impact on surface runoff

Comparing the differences of monthly potential evapotranspiration, surface evapotranspiration and precipitation in spruce forests (Table 2), the results clearly showed that rainfall fluctuated between 0-16mm, and the maximum rainfall was 15.7 mm in April, while the minimum value of surface evapotranspiration is 41.8 mm and the minimum value of potential evapotranspiration is 44.1mm. The huge difference between ET_P and ET shows that there is no effective water accumulation in all months. From this, an important conclusion can be drawn: surface runoff can not be collected in this area, which also proves that afforestation in this area will further enhance evapotranspiration, posing a threat to water distribution and utilisation.

Table 2 Month-by-month comparison of potential evapotranspiration, surface evapotranspiration and rainfall

Month / Variable	4	5	6	7	8	9	10
ET_p/mm	76.6	87.6	106.5	128.3	118.1	80.0	44.1
ET/mm	51.5	66.3	93.3	108.9	110.7	81.2	41.8
P/mm	15.7	8.8	0	13.2	13.3	11.2	13.6

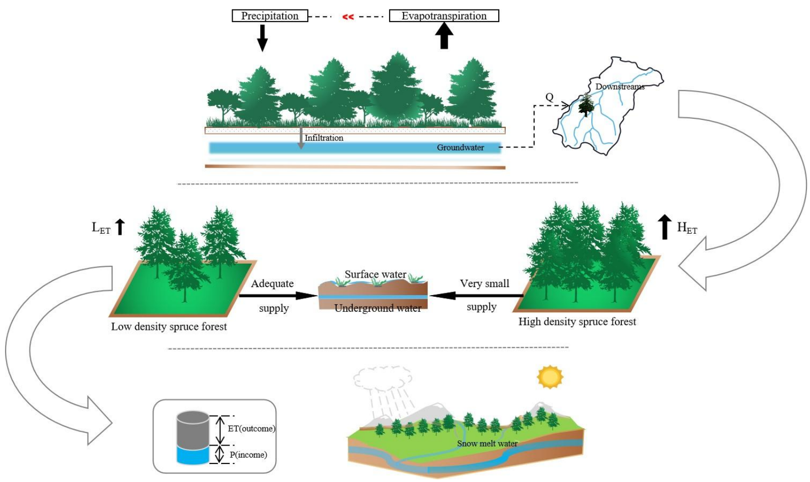

Figure 6 Conceptual model of the hydrological effects of changes in evapotranspiration

Some studies suggested that reducing forest density will result in less ET in seasonally dry forests. That reduced ET can be converted into increased groundwater and runoff to supply downstream social water (Wyatt, O'Donnell, & Springer, 2015). It has also been claimed that in some cases, the transient increase in water availability through reduced forest density can actually contribute to subsequent increases in vegetation cover and ultimately reduce runoff (Tague et al., 2019). By assessing the hydrological effects of afforestation through the water cycle in the Asia-Pacific region, it was found that in 7 of the 15 water-deficient areas, positive effects such as increased yield, precipitation, soil moisture and reduced drought risk were achieved through afforestation, and it was confirmed that the water-water cycle had a strong impact and EVapotranspiration was increased (Teo et al., 2021). The water vapour content consumed by forest transpiration is much higher than that lost by soil surface evaporation, most of the precipitation is intercepted and infiltrated by surface vegetation, and part of the soil water involved in infiltration is absorbed by the root zone of vegetation(Fig. 6). Because of plants' high interception and evaporation ability and the absorption of groundwater by root zone, the proportion of transpiration was significantly higher than that of evaporation(Su et al., 2014). In this case, the groundwater amount decreases gradually with the T value increase. Under the influence of precipitation loss mainly due to plant transpiration, groundwater yield in this region decreases greatly, and has no significant contribution to the downstream water revenue.

5.1.2 Contribution to recirculating water vapour in precipitation

In the Qilian Mountains, the contribution of circulating water to precipitation is often higher in areas above 2400 m above sea level than in the foothills (2100-2400 m above sea level), and the contribution of transpiration water from plants is also higher than that of surface evaporation contribution of f_{tr} moisture to precipitation is higher in mountainous areas than in f_{ev}, and the contribution of circulating moisture increases with increasing altitude (Zhang et al., 2022; Zhang et al., 2021). The proportional contribution of circulating water vapour (surface evaporation and transpiration water vapour) to precipitation in Qinghai spruce forests from 2017 to 2019 was assessed using a three-component model (Fig. 7), and the results showed that the contribution of plant transpiration water vapour in summer was larger than the values in the other two seasons, and excluding the contribution of advection water vapour, plant transpiration water vapour was higher than the contribution of surface evaporation water vapour, and this result revealed that in eastern Qilian Mountains, evapotranspiration from spruce forests is the main mode of precipitation consumption in the local water cycle. The assessment of mountain, oasis and desert areas in inland river basins in the monsoonal marginal zone found that advective water vapour contributions consistently dominate precipitation, yet plant transpiration and surface evaporation are closely related to temperature changes during the local water vapour cycle (Zhu et al., 2019).

https://doi.org/10.5194/hess-2022-375
Preprint. Discussion started: 16 January 2023

Hydrology and Earth System Sciences
Open Access
Discussions

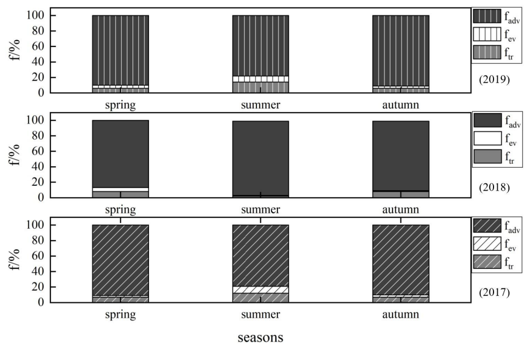

Figure 7 Comparison of f_{adv} (advective water vapour contribution), f_{ev} (surface evaporation water vapour contribution) and f_{tr} (plant transpiration water vapour contribution) for each of the spring, summer and autumn seasons 2017-2019

5.1.3 Impact on soil moisture

Water stress is an essential factor affecting the growth of spruce forests. Water in the soil will affect the transpiration of the leaf surface, and too little water will reduce carbon dioxide, thus reducing photosynthesis. The temporal variation of water content in the basal layer of Qinghai spruce at an altitude of 2721 m and the temporal variation of transpiration components in the spruce forest ecosystem during the same period were matched to reflect the interrelationship between the two. The water content of the shallow soil layer at 0-10 cm decreased slightly from April to June, then increased to 49.84% from June to September and decreased slightly from September to October. The water content of other soil layers in the vertical profile showed consistent changes with that of the shallow soil layer. Overall, the SWC was higher in April and May as a result of abundant rainfall and then decreased until June, when it gradually showed an elevated rate of increase in soil water content from June onwards.

The effect of SWC on T/ET showed some lag in time. Figure 8 reflected that T/ET changed in an increasing, decreasing, and then increasing trend from April to

https://doi.org/10.5194/hess-2022-375
Preprint. Discussion started: 16 January 2023

August, while shallow soil water content showed slight changes from April to June and gradually grew and then fell from June to September. They show a roughly parallel correlation with a slight lag. For natural ecosystems, the results of the intermittent studies showed higher variability than those of the long-term studies. The range of long-term T/ET variability is narrower, with a mean value of 0.52, demonstrating that soil evaporation and plant transpiration in natural drylands are essentially equivalent over the long term. Agroecosystems typically exhibit relatively high T/ET, and natural and agroecosystems have approximately the same T/ET maximum(Li et al., 2022; Gao et al., 2018). During dynamic wet and dry processes, soil evaporation and plant transpiration respond differently in terms of time and duration. Soil evaporation is more controlled by meteorological processes and shallow soil moisture, while transpiration is more controlled by plant phenology and water effectiveness in the root zone(Sun et al., 2019; Li et al., 2014).

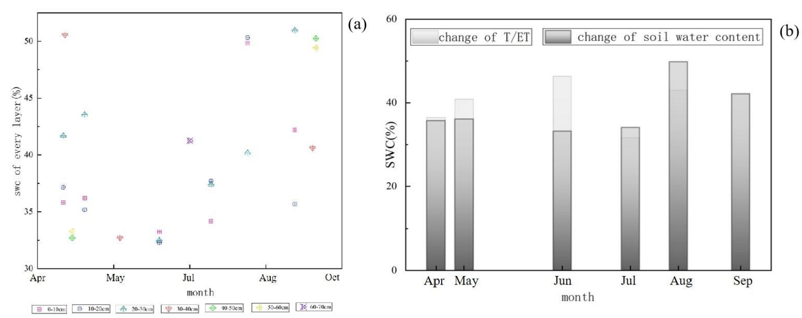

Figure 8 Soil water content and ecosystem evapotranspiration

5.2 Impact of climate change on evapotranspiration in Qinghai spruce forests

Temperature exerts an influence on vegetation physiological activity through its effect on moisture and enzyme activity within the vegetation, while relative humidity also has an immediate bearing on the liquid water isotopic composition of the soil surface (Fig. 9). Thus, both temperature and relative humidity are important influences on the partitioning of evapotranspiration. Temperature generally tends to be higher from April to August, with the monthly mean

https://doi.org/10.5194/hess-2022-375
Preprint. Discussion started: 16 January 2023

Hydrology and Earth System Sciences
Discussions

temperature reaching a six-month maximum in August, rising to 14°C, while the temperature drops rapidly in the next two months to 3°C, with the temperature dropping monthly by 6°C in April. Relative humidity increases roughly from April to June, with slight movements from June to July, before the relative humidity value fluctuates up to 72.43%, an increase of about 18% compared to April. Season-wise, the temperature is markedly elevated in the monsoon season, whereas the relative humidity is greater in the monsoon season than in April and May and weaker than in September and October. It can be deduced that relative humidity drives the ecosystem T/ET ratio more sharply during the summer wind-influenced phase and exhibits a combination of temperature and relative humidity variability in the other seasons.

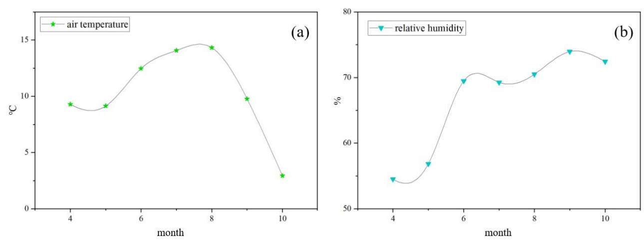

Figure 9 Variation in temperature and relative humidity

6. Conclusions

This paper utilizes isotope data combined with model simulations to elucidate the link between evapotranspiration and the local water cycle in the study area and their hydrological effects. The results showed that July and August were the peak periods of spruce growth, and the evapotranspiration and transpiration intensity were both high. Compared with each other, the transpiration intensity of spruce was higher than that of soil evaporation. Further specific quantification of plant transpiration and soil evaporation on the proportion of evapotranspiration results showed that the mean value of f_T was 79% and the mean value of f_E was 20%. The contribution of plant transpiration was much higher than that of soil evaporation. The analysis of the hydrological effects of evapotranspiration in spruce forest belts revealed that evapotranspiration was greater than precipitation in all months, making it difficult to develop surface runoff reliant on precipitation. In the context of global warming, climate drivers may change the ecological communities, ecosystem functions, and land-climate interactions of spruce forests. Some policies implemented in China, such as returning farmland to forest, ecological red line and national park construction, may lead to changes in the distribution region and area of the Qinghai spruce forest. Therefore, research and assessment of the ecohydrological implications of forest change in drylands should be continued.

Acknowledgements

This research was financially supported by the National Natural Science Foundation of China (41867030, 41971036). The authors much thank the colleagues in the Northwest Normal University for their help in fieldwork, laboratory analysis, data processing.

Data availability statement

The data that support the findings of this study are available on request from the corresponding author, stable isotope data are not publicly available due to privacy or ethical restrictions. Potential evapotranspiration and surface evapotranspiration data are available from the National Tibetan Plateau Scientific Data Centre(TPDC).

Competing Interests

We undersigned declare that this manuscript entitled “Hydrological effects of evapotranspiration in the Qilian Mountains forest belt” is original, has not been published before and is not currently being considered for publication elsewhere.

The authors declare that they have no known competing financial interests or personal relationships that could have appeared to influence the work reported in this paper.

References

Anderegg W R L, Kane J M, Anderegg L D L. Consequences of widespread tree mortality triggered by drought and temperature stress[J]. Nature climate change, 2013, 3(1): 30-36.

Ault T R. On the essentials of drought in a changing climate[J]. Science, 2020, 368(6488): 256-260.

Chang Y, Ding Y, Zhang S, et al. Dynamics and environmental controls of evapotranspiration for typical alpine meadow in the northeastern Tibetan Plateau[J]. Journal of Hydrology, 2022, 612: 128282.

Chen H, Zhu G, Shang S, et al. Uncertainties in partitioning evapotranspiration by two remote sensing-based models[J]. Journal of Hydrology, 2022, 604: 127223.

Cui Y, Jia L, Fan W. Estimation of actual evapotranspiration and its components in an irrigated area by integrating the Shuttleworth-Wallace and surface temperature-vegetation index schemes using the particle swarm optimization algorithm[J]. Agricultural and Forest Meteorology, 2021, 307: 108488.

Díaz S, Kattge J, Cornelissen J H C, et al. The global spectrum of plant form and function[J]. Nature, 2016, 529(7585): 167-171.

Ding, Y.X., & Peng, S.Z. (2020). Spatiotemporal trends and attribution of drought across China from 1901–2100. Sustainability, 12(2), 477.

Ding, Y.X., Peng, S.Z. (2021). Spatiotemporal change and attribution of potential evapotranspiration over China from 1901 to 2100. Theoretical and Applied Climatology. https://doi.org/10.1007/s00704-021-03625-w.

Eisenhauer N, Weigelt A. Ecosystem effects of environmental extremes[J]. Science, 2021, 374(6574): 1442-1443.

Gao, C. J. (2018). Regional differences in land-atmosphere coupling and possible impacts of soil moisture over Eastern China. Nanjing University of Information Science & Technology (In Chinese).

Han J, Tian L, Cai Z, et al. Season-specific evapotranspiration partitioning using dual water isotopes in a Pinus yunnanensis ecosystem, southwest China[J]. Journal of Hydrology, 2022, 608: 127672.

Keeling C D. The concentration and isotopic abundances of atmospheric carbon dioxide in rural areas[J]. Geochimica et cosmochimica acta, 1958, 13(4): 322-334.

Kool D, Agam N, Lazarovitch N, et al. A review of approaches for evapotranspiration partitioning[J]. Agricultural and forest meteorology, 2014, 184: 56-70.

Li Q, Ye A, Zhang Y, et al. The peer-to-peer type propagation from meteorological drought to soil moisture drought occurs in areas with strong land-atmosphere interaction[J]. Water Resources Research, e2022WR032846.

Li X, Liang S, Yuan W, et al. Estimation of evapotranspiration over the terrestrial ecosystems in China[J]. Ecohydrology, 2014, 7(1): 139-149.

Liu Y, Zhuang Q, Miralles D, et al. Evapotranspiration in Northern Eurasia: Impact of forcing uncertainties on terrestrial ecosystem model estimates[J]. Journal of Geophysical Research: Atmospheres, 2015, 120(7): 2647-2660.

Maxwell R M, Condon L E. Connections between groundwater flow and transpiration Partitioning [J]. Science, 2016, 353(6297): 377-380.

Peng W L, Zhao L J, Xie C, et al. Et segmentation of Picea Qinghai forest ecosystem in the upper reaches of Heihe River [J]. Journal of Glaciology and Geocryology, 2020, 42(2): 629-640.

Peng, S. (2022). 1 km monthly potential evapotranspiration dataset in China (1990-2021). National Tibetan Plateau Data Center, 2022. DOI: 10.11866/db.loess.2021.001.

Peng, S.Z., Ding, Y.X., Liu, W.Z., & Li, Z. (2019). 1 km monthly temperature and precipitation dataset for China from 1901 to 2017. Earth System Science Data, 11, 1931–1946. https://doi.org/10.5194/essd-11-1931-2019.

Peng, S.Z., Ding, Y.X., Wen, Z.M., Chen, Y.M., Cao, Y., & Ren, J.Y. (2017). Spatiotemporal change and trend analysis of potential evapotranspiration over the Loess Plateau of China during 2011-2100. Agricultural and Forest Meteorology, 233, 183-194. https://doi.org/10.1016/j.agrformet.2016.11.129.

Raz-Yaseef N, Rotenberg E, Yakir D. Effects of spatial variations in soil evaporation caused by tree shading on water flux partitioning in a semiarid pine forest[J]. Agricultural and Forest Meteorology, 2010, 150(3): 454-462.

Rohatyn S, Yakir D, Rotenberg E, et al. Limited climate change mitigation potential through forestation of the vast dryland regions[J]. Science, 2022, 377(6613): 1436-1439.

Schlesinger W H, Jasechko S. Transpiration in the global water cycle[J]. Agricultural and Forest Meteorology, 2014, 189: 115-117.

Su T, Lu Z Y, Zhou J, et al. Spatial distribution and seasonal variation characteristics of global atmospheric moisture recycling[J]. 2014.

Sun X, Wilcox B P, Zou C B. Evapotranspiration Partitioning in dryland ecosystems: A global meta-analysis of in situ studies[J]. Journal of Hydrology, 2019, 576: 123-136.

Tague CL, Moritz M, Hanan E. The changing water cycle: The eco-hydrologic impacts of forest density reduction in Mediterranean (seasonally dry) regions. WIREs Water. 2019;e1350. https://doi.org/10.1002/wat2.1350

Talsma C J, Good S P, Jimenez C, et al. Partitioning of evapotranspiration in remote sensing-based models[J]. Agricultural and Forest Meteorology, 2018, 260: 131-143.

Teo H C, Raghavan S V, He X, et al. Large-Scale Reforestation Can Increase Water Yield and Reduce Drought Risk for Water-Insecure Regions in the Asia-Pacific[J]. Available at SSRN 3989861.

Wang L, Good S P, Caylor K K. Global synthesis of vegetation control on evapotranspiration partitioning[J]. Geophysical Research Letters, 2014, 41(19):

https://doi.org/10.5194/hess-2022-375
Preprint. Discussion started: 16 January 2023

6753-6757.

Wei Z, Lee X, Wen X, et al. Evapotranspiration partitioning for three agroecosystems with contrasting moisture conditions: a comparison of an isotope method and a two-source model calculation[J]. Agricultural and Forest Meteorology, 2018, 252: 296-310.

Wershaw, R.L., Friedman, I., Heller, S.J., Frank, P.A., 1966. Hydrogen isotope fractionation of water passing through trees. In: Hobson, G.D. (Ed.), Advances in OrganicGeochemistry. Pergamon Press, New York, pp. 55–67.

Wyatt, C. J. W., O'Donnell, F. C., & Springer, A. E. (2015). Semi-Arid Aquifer Responses to Forest Restoration Treatments and Climate Change.Groundwater, 53(2), 207–216.

Yao Y., Liang S., Li X., Chen J., Liu S., et al. Improving global terrestrial evapotranspiration estimation using support vector machine by integrating three process-based algorithms. Agricultural and Forest Meteorology 2017, 242, 55-74. DOI: 10.1016/j.agrformet.2017.04.011.

Yao, Y., Liu, S., Shang, K. (2020). Daily MODIS-based Land Surface Evapotranspiration Dataset of 2019 in Qilian Mountain Area (ETHi-merge V1.0). National Tibetan Plateau Data Center, 2020. DOI: 10.11888/Meteoro.tpdc.270407.

Yepez E A, Huxman T E, Ignace D D, et al. Dynamics of transpiration and evaporation following a moisture pulse in semiarid grassland: A chamber-based isotope method for partitioning flux components[J]. Agricultural and Forest Meteorology, 2005, 132(3-4): 359-376.

Yong L, Zhu G, Wan Q, et al. The soil water evaporation process from mountains based on the stable isotope composition in a headwater basin and northwest China[J]. Water, 2020, 12(10): 2711.

Zhang R, Xu X, Liu M, et al. Comparing evapotranspiration characteristics and environmental controls for three agroforestry ecosystems in a subtropical humid karst area[J]. Journal of hydrology, 2018, 563: 1042-1050.

https://doi.org/10.5194/hess-2022-375
Preprint. Discussion started: 16 January 2023

Zhang Y, Gentine P, Luo X, et al. Increasing sensitivity of dryland vegetation greenness to precipitation due to rising atmospheric CO^2[J]. Nature communications, 2022, 13(1): 1-9.

Zhang Z, Zhu G, Pan H, et al. Quantifying recycled moisture in precipitation in Qilian Mountains[J]. Sustainability, 2021, 13(23): 12943.

Zhu G, Guo H, Qin D, et al. Contribution of recycled moisture to precipitation in the monsoon marginal zone: Estimate based on stable isotope data[J]. Journal of Hydrology, 2019, 569: 423-435.

Zhu G, Guo H, Qin D, et al. Contribution of recycled moisture to precipitation in the monsoon marginal zone: Estimate based on stable isotope data[J]. Journal of Hydrology, 2019, 569: 423-435.

Zhu G, Liu Y, Shi P, et al. Stable water isotope monitoring network of different water bodies in Shiyang River basin, a typical arid river in China[J]. Earth System Science Data, 2022, 14(8): 3773-3789.